Ferrous Iron Under Oxygen-Rich Conditions in the Deep Mantle

E. Boulard, M. Harmand, F. Guyot, G. Lelong, Guillaume Morard, D. Cabaret, S. Boccato, A D Rosa, R. Briggs, S. Pascarelli, et al.

Ferrous Iron Under Oxygen-Rich Conditions in the Deep Mantle

E. Boulard[1] [iD], M. Harmand[1] [iD], F. Guyot[1], G. Lelong[1], G. Morard[1] [iD], D. Cabaret[1], S. Boccato[1,2] [iD], A. D. Rosa[2], R. Briggs[2,3] [iD], S. Pascarelli[2], and G. Fiquet[1]

[1]Sorbonne Université, Muséum National d'Histoire Naturelle, UMR CNRS 7590, IRD, Institut de Minéralogie, Physique des Matériaux et Cosmochimie - IMPMC, 4 Place Jussieu, 75005 Paris, France, [2]European Synchrotron Radiation Facility, Grenoble, France, [3]Now at Lawrence Livermore National Laboratory, Livermore, California, USA

Abstract Recent experiments have demonstrated the existence of previously unknown iron oxides at high pressure and temperature including newly discovered pyrite-type FeO_2 and FeO_2H_x phases stable at deep terrestrial lower mantle pressures and temperatures. In the present study, we probed the iron oxidation state in high-pressure transformation products of $Fe^{3+}OOH$ goethite by in situ X-ray absorption spectroscopy in laser-heated diamond-anvil cell. At pressures and temperatures of ~91 GPa and 1,500–2,350 K, respectively, that is, in the previously reported stability field of FeO_2H_x, a measured shift of -3.3 ± 0.1 eV of the Fe K-edge demonstrates that iron has turned from Fe^{3+} to Fe^{2+}. We interpret this reductive valence change of iron by a concomitant oxidation of oxygen atoms from O^{2-} to O^-, in agreement with previous suggestions based on the structures of pyrite-type FeO_2 and FeO_2H_x phases. Such peculiar chemistry could drastically change our view of crystal chemistry in deep planetary interiors.

Plain Language Summary Iron oxides are important end-members of the complex materials that constitute the Earth's interior. Among them, FeO and Fe_2O_3 have long been considered as the main end-members of the ferrous (Fe^{2+}) and ferric (Fe^{3+}) states of iron, respectively. All geochemical models assume that high oxygen concentrations are systematically associated to the formation of ferric iron in minerals. The recent discovery of O_2^{2-} peroxide ions in a phase of chemical formula FeO_2H_x stable under high-pressure and high-temperature conditions challenges this general concept. However, up to now, the valences of iron and oxygen in FeO_2H_x have only been indirectly inferred from a structural analogy with pyrite FeS_2. Here we compressed goethite (FeOOH), an Fe^{3+}-bearing mineral, at lower mantle pressure and temperature conditions by using laser-heated diamond-anvil cells, and we probed the iron oxidation state upon transformation of FeOOH in the pressure–temperature stability field of FeO_2H_x using in situ X-ray absorption spectroscopy. The data demonstrate that upon this transformation iron has transformed into ferrous Fe^{2+}. Such reduced iron despite high oxygen concentrations suggests that our current views of oxidized and reduced species in the lower mantle of the Earth should be reconsidered.

1. Introduction

Iron oxides are important end-members of the complex materials that constitute the Earth's interior. Among them, wüstite (FeO) and hematite (Fe_2O_3) have been considered for long as the two main end-members for the ferrous (Fe^{2+}) and ferric (Fe^{3+}) states of iron, respectively. Magnetite (Fe_3O_4) has a well-defined mixed ferrous and ferric valence with a ratio of 1:2. Recent studies, however, have reported the existence under high pressures (*P*) and temperatures (*T*) of new stoichiometries such as Fe_4O_5, Fe_5O_6, and Fe_7O_9 (Lavina et al., 2011; Lavina & Meng, 2015; Sinmyo et al., 2016), in which iron valences are not yet known. The recent discovery of a new iron peroxide FeO_2 under lower mantle *P*–*T* conditions may drastically change our understanding of iron crystal chemistry and geochemistry in deep planetary mantles (Hu et al., 2016). Indeed, if FeO_2 is isostructural and isochemical with FeS_2 pyrite, as proposed in Hu et al. (2016), iron would be ferrous despite the large oxygen concentrations under which it was synthesized.

FeO_2 was first investigated with both first-principle calculations and experiments by Hu et al. (2016) who reported the reaction between Fe_2O_3 and O_2 at *P*–*T* conditions corresponding to a depth of ~1,800 km in the Earth (76 GPa–1,500 K). FeO_2 presents the same crystal structure as pyrite FeS_2: an Fe atom surrounded by six O atoms makes slightly distorted FeO_6 octahedra with an Fe–O average bond length of ~1.808 Å. Due to the presence of O–O covalent bonds, oxygen atoms in this new phase would have a valence of −1 (as in

AGU
100
ADVANCING EARTH
AND SPACE SCIENCE

Geophysical Research Letters

10.1029/2019GL081922

peroxide anions O_2^{-2}) and consequently iron would present a valence of +2 (Hu et al., 2016). If this proposed valence of iron in FeO_2 is confirmed, the stability of Fe^{2+} under high oxygen fugacity would drastically modify our understanding of oxidation state and redox reactions that take place within the Earth's lowermost mantle. Current models indeed assume that a high oxygen fugacity and oxidizing conditions are systematically associated to the formation of Fe^{3+}, and in turn, Fe^{3+}/Fe^{2+} ratios are used for oxygen fugacity calculations. With the presence of peroxide ions, mantle redox states would need to be reconsidered. However, up to now, the valences of iron and oxygen in FeO_2 are still under debate and are only indirectly suggested by the structural analogy with pyrite FeS_2. The reported O–O distance of 1.89 Å in FeO_2 (Hu et al., 2016), as inferred from atomic position refinements, is larger than in molecular oxygen (1.21 Å) and in O_2^{-2} peroxide ion as in BaO_2 and MgO_2 (1.49 and 1.45 Å, respectively; Koigstein et al., 1998; Lobanov et al., 2015; Streltsov et al., 2017). On this basis, one may instead expect that Fe ion in FeO_2 would adopt an exceptionally high oxidation state of +4, as in oxoiron (IV) compounds well known in biology and chemistry. Theoretical calculations based on the combination of density functional and dynamical mean-field theories have also proposed intermediate valences of Fe^{3+} and $O^{-1.5}$ in the newly discovered FeO_2 phase (Streltsov et al., 2017).

Pyrite-structured iron peroxides were also synthetized starting from a common hydrous ferric mineral, α-FeOOH goethite (Boulard et al., 2018; Hu et al., 2017, 2016; Nishi et al., 2017; Zhu et al., 2017), or by reaction between Fe and H_2O (Liu et al., 2017; Mao et al., 2017; Yuan et al., 2018) as well as by reaction between Fe_2O_3 and H_2O (Hu et al., 2017; Liu et al., 2017; Mao et al., 2017). However, because the pyrite-structured phases synthesized in these studies have variable and larger unit cells than in FeO_2 under the same conditions, it was suggested that FeOOH transformed into pyrite-structured FeO_2H_x with x values comprised between 0.4 and 1 (Boulard et al., 2018; Hu et al., 2017; Nishi et al., 2017). In the transformation process from FeOOH to FeO_2H_x, H_2 or equivalent zero-valent hydrogen could be released (Hu et al., 2017), impacting the global hydrogen and water geochemical cycles. One should note, however, that there are strong divergences about the actual hydrogen content of pyrite-structured FeO_2H_x. Complete dehydrogenation of FeOOH into FeO_2 was initially suggested to occur at mantle conditions (Hu et al., 2016). More recently, Hu et al. (2017) and Boulard et al. (2018) advocated for a partial dehydrogenation while Nishi et al. (2017) reported no loss of H in the transformation of FeOOH. In that last scenario, one could expect the iron oxidation state to be Fe^{3+} as in α-FeOOH, together with H^{+1} hydrogen and O^{-2} oxygen, that is, a high-pressure $Fe^{3+}O^{2-}(OH)^-$ hydrous polymorph of goethite with a pyrite structure containing iron, oxygen, and hydrogen with usual valences. However, if peroxide anions are involved, Fe^{2+} would also be compatible with a goethite formula as in $Fe_2^{2+}O_2^{2-}(OH)_2^-$.

To shed light on the valence states of iron in high-pressure transformation products of goethite $Fe^{3+}OOH$, we used X-ray Absorption Near Edge Structure (XANES) at the Fe K-edge in situ at high pressure and temperature. Indeed, preedge features in the Fe K-edge absorption spectra and the edge position itself are well known to be related to Fe^{2+}/Fe^{3+} ratio and are now commonly used to determine the valence states of a wide variety of minerals (e.g., Wilke et al., 2001). Analyses were performed in a laser-heated diamond-anvil cell at high pressure and temperature upon the transformation of FeOOH in the previously reported stability field of FeO_2H_x. The same methodology was applied on pure FeO and Fe_2O_3, which were used as reference samples for Fe^{2+} and Fe^{3+} oxides, respectively.

2. Materials and Methods

Starting materials consisted of a natural sample of crystalline goethite (α-FeOOH) from a lateritic soil of Central African Republic provided by the collection of University Pierre et Marie Curie. Pellets of α-FeOOH were loaded in diamond anvil cells (DAC) either in neon (Ne) gas or between two dry potassium chloride (KCl) disks. Ne and KCl acted both as pressure media as well as thermal insulators. Complementary high-pressure and high-temperature experiments were performed on the two end-member oxides, α-$Fe^{3+}_2O_3$ and $Fe^{2+}O$, which served as references for the two iron valence states at high pressure and temperature. To our knowledge, no previous XANES data exist on FeO and Fe_2O_3 at both high-pressure and high-temperature conditions. For these experiments, we used synthetic starting materials purchased from Sigma-Aldrich with >99.9 and 99.7% purity, respectively, loaded in-between oven-dried KCl disks.

X-ray absorption spectroscopy measurements at the Fe K-edge were performed at the beamline ID24 of the European Synchrotron Radiation Facility (Kantor et al., 2014, 2018; Pascarelli et al., 2016). XANES spectra were collected in situ at high pressure and temperature by coupling a DAC and a double-sided laser heating setup. For each sample, XANES spectra were first collected during compression at ambient temperature, then in situ at high pressure and temperature and after quench to ambient temperature. Due to the X-ray absorption setup used, no simultaneous X-ray diffraction could be performed; we thus assume the phases present from previous X-ray diffraction measurements on the same assemblages and at the same pressure and temperature conditions (e.g., Bykova et al., 2016; Fischer et al., 2011; Hu et al., 2016). Extended description of the experimental methods and spectrum analysis can be found in the supporting information (Akahama & Kawamura, 2004; Benedetti & Loubeyre, 2004; Boccato et al., 2017; Boubnov et al., 2015; Dewaele et al., 2008; Dräger et al., 1988; Galoisy et al., 2001; Giampaoli et al., 2018; Waychunas et al., 1983; Max Wilke et al., 2005).

3. Results

3.1. Compression at Ambient Temperature of α-FeOOH

XANES spectra collected during compression at ambient temperature of FeOOH goethite loaded into Ne are shown in Figure 1. The XANES features of the Fe K-edge collected at 14 GPa are in good agreement with the literature related to Fe K-edge of α-FeOOH (Piquer et al., 2014; Wilke et al., 2001), which is the thermodynamically stable phase at ambient conditions. As expected for slightly distorted octahedrally coordinated Fe^{3+}, the preedge presents two main features near 7,113 and 7,115 eV associated with electronic transitions to the t_{2g} and e_g empty Fe 3d orbitals, respectively (Wilke et al., 2001). The crystal field splitting energy obtained from the splitting between the two preedge features shows a linear increase from 1.6 at 14 GPa up to 2.1 eV at 39 GPa interpreted as due to the compression of FeO_6 octahedra with pressure. In the meantime, the preedge's centroid is observed to move toward lower energies: from 7,114.8 eV at 33 GPa to 7,114.0 eV at 64 GPa (Figure S2). The white line of the edge is also modified with the appearance of a shoulder around 7,124 eV for pressures above 33 GPa, and the feature A is shifted by +3 eV (Figure 1).

Compressibility of α-FeOOH at ambient temperature has been previously studied by X-ray diffraction, and it is known that α-FeOOH undergoes an iso-structural phase transition at ~49 GPa upon the spin-crossover of iron from high spin (HS) to low spin (LS), a pressure-induced electronic process that is accompanied by hydrogen bond symmetrization and FeO_6 octahedra becoming regular (Gleason et al., 2013; Reagan et al., 2016; Xu et al., 2013). Since the preedge feature is sensitive to the t_{2g} and e_g components of the 3d band through hybridization effects, it is directly connected to the population of the HS and LS spin states. Here modifications in the preedge and edge XANES features between 33 and 39 GPa at ambient temperature show similarities with data collected upon the Fe spin transition in Fe_2O_3 (Figure S3; Badro et al., 2002; Mao et al., 1996; Narygina et al., 2009; Sanson et al., 2016; Wang et al., 2010). Therefore, we attribute the modifications of the preedge observed in this pressure range to the pressure-induced iron spin-crossover in α-FeOOH. These compression data show that Fe^{2+}/Fe^{3+} quantitative analysis of the preedge centroid position and intensity as developed by Wilke et al. (2001) is not systematically possible due to the structural and/or spin transition and related modifications in the preedge at high pressures. However, this does not prevent qualitative and unambiguous observation of the valence state evolution.

3.2. Transformation Into ε-FeOOH at ~64 GPa and 1,600–1,800 K

α-FeOOH was pressurized up to ~64 GPa in Ne and transformed by laser heating at temperatures of ~1,600 K. The corresponding XANES Fe K-edge spectra collected before and after heating are presented in Figure 2. Table S1 summarizes the spectral positions of the main Fe K-edge features of FeOOH, FeO, and Fe_2O_3 before and after laser heating at 64 GPa. Within a few seconds of laser heating, the A spectral feature of the XANES spectra was shifted toward higher energies (by about +1 eV). The flank of the edge and feature B were also modified. The position of the white line did not evolve but the centroid position of the preedge shifted from 7,114.0 to 7,114.4 eV (Figure S2). Further heating up to 1,800 K at this pressure condition and then temperature quenching did not result in any significant changes. The modification of the XANES Fe K-edge spectra at ~64 GPa and 1,600–1,800 K is to be related to the transformation of α-FeOOH into ε-FeOOH, a rutile-type structure that has been reported to occur at these P–T conditions (Gleason et al., 2008; Suzuki, 2010; Figure 2).
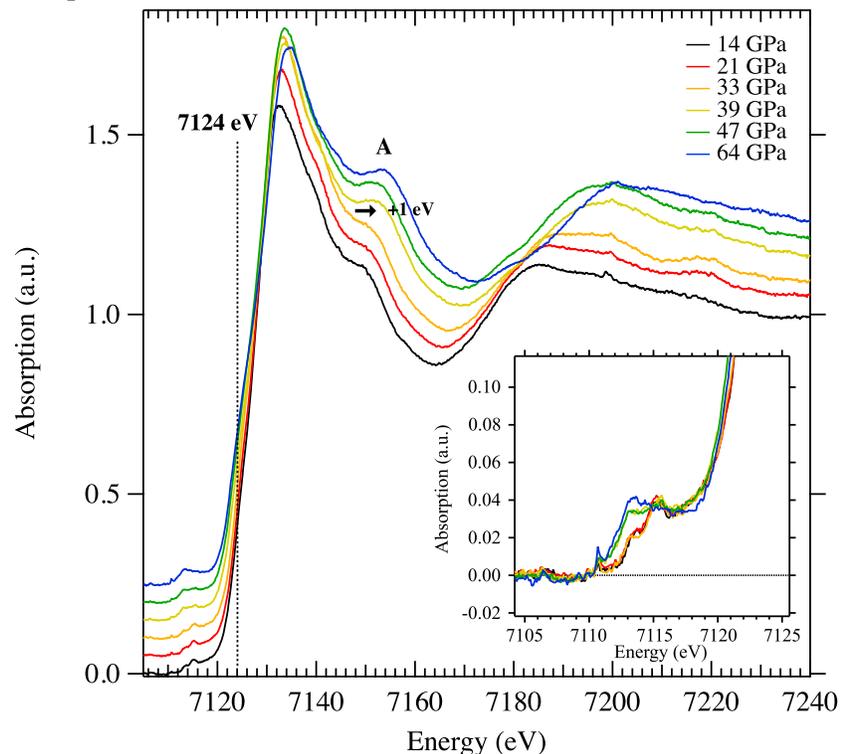
Figure 1. Normalized Fe-K edge XANES spectra collected upon compression up to 64 GPa at ambient temperature of FeOOH loaded into neon. Inset: pre-edge area of the spectra.

For comparison, XANES spectra were collected on FeO at 47 GPa (ambient temperature) and on Fe_2O_3 at 54 GPa and ~1,500–2,000 K. The edge positions of FeOOH and Fe_2O_3 after laser heating are close to each other and ~4 eV higher than the Fe K-edge position in FeO (Figure 2 and Table S1). Using in situ Mössbauer spectroscopy at high pressure, Bykova et al. (2016) have reported that iron in η-Fe_2O_3, the stable polymorph of Fe_2O_3 at these conditions, is indeed Fe^{3+}. Therefore, we can conclude that iron is also in a Fe^{3+} valence state in ϵ-FeOOH.

3.3. Transformation Into FeO_2H_x at ~91 GPa and 1,500–2,350 K

FeOOH was compressed at ambient temperature directly at 91 GPa in KCl and at 87 GPa in neon, respectively, before transformation under laser heating at temperatures ranging from 1,500 to 2,350 K. As presented in Figure 3, drastic changes in the XANES spectra are observable. In addition to the modifications of postedge features, a clear shift of the edge by about 3.3 eV toward lower energies took place together with a −2-eV shift of the maximum intensity position of the XANES spectrum. We observed no evidence of a shift in the centroid position of the preedge, which remained at about 7,114 eV (Figure S2). Again, these modifications in the Fe K-edge XANES were observed within a few seconds of laser heating at 1,800 K and no evolution occurred in the spectra upon heating over longer durations or at higher temperatures, up to 2,350 K.

The −3.3-eV energy shift of the absorption threshold that is observed at ~90 GPa and 1,500–2,350 K is consistent with a change in oxidation state of the Fe ions from Fe^{3+} to Fe^{2+}. The new edge position is indeed close to that in $Fe^{2+}O$ at the same P–T conditions and about 4.5 eV below that of the edge position in $Fe^{3+}_2O_3$ (Figures 3 and S4; Bykova et al., 2016; Fischer et al., 2011; Ozawa et al., 2010) and below the edge position expected for an oxoiron (Fe^{4+})-bearing phases (e.g., England et al., 2014; Rohde et al., 2004). Postedge features are different from those of FeO; the synthetized phase is therefore different from wüstite. Moreover, several previous experimental (X-ray diffraction) and theoretical studies have shown that at these pressure and temperature, FeOOH transforms into the pyrite-structured FeO_2H_x phase (Boulard
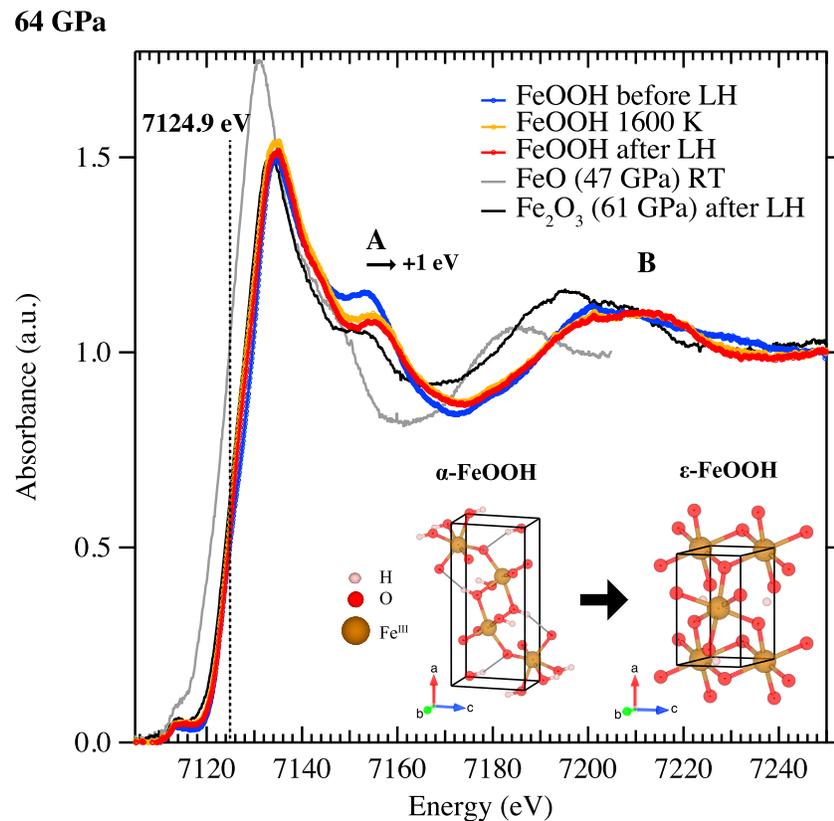
Figure 2. Normalized Fe-K edge XANES spectra collected at ~64 GPa before, during, and after laser heating (LH) of FeOOH loaded into neon. For comparison, spectra collected in FeO and Fe_2O_3 at similar pressure and temperature conditions are also shown. RT: room temperature. As α-FeOOH transforms in to the high-pressure polymorph ϵ-FeOOH (Pernet et al., 1975), the Fe-K edge position remains at ~7,124.9 eV.

et al., 2018; Hu et al., 2017, 2016; Nishi et al., 2017). Our results therefore suggest that in FeO_2H_x, part of the FeO_6 octahedra are connected by O–O bonds resulting in the formation of the peroxide dimer O_2^{2-}. This observation agrees with previous experimental and theoretical work who suggested the presence of O^{1-} and Fe^{2+} in this P–T range of the Fe–O–H phase diagram (Boulard et al., 2018; Hu et al., 2017, 2016; Jang et al., 2017; Mao et al., 2017). This observation would also be consistent with the release of H as zerovalent hydrogen from symmetrically hydrogen-bonded ϵ-FeOOH upon transformation to the pyrite-structured FeO_2H_x according to reaction (1) as reported by Zhu et al. (2017).

$$Fe^{3+}OOH -> Fe^{2+}O_2H_x + (1-x)/2 \ H_2 \tag{1}$$
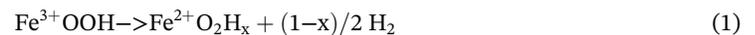
We stress, however, that the present XANES measurements do not give any direct insight on the actual hydrogen content in the high-pressure phases studied. A $Fe_2^{2+}O_2^{2-}(OH)_2^-$ phase with no H loss with respect to a goethite composition would be equally consistent with the X-ray absorption data of the present study.

4. Implications

Here we report unambiguous observation of Fe^{2+} in high-pressure high-temperature transformation products of $Fe^{3+}OOH$ goethite at ~91 GPa and 1,500–2,350 K. Although we could not get a structural determination of the phase simultaneously to the measurement of the X-ray absorption, we notice that at least three experimental studies carried out under similar or identical conditions obtained a pyrite-structured FeO_2H_x phase (x comprised between 0.4 and 1) in this region of the Fe–O–H phase diagram (Boulard et al., 2018; Hu
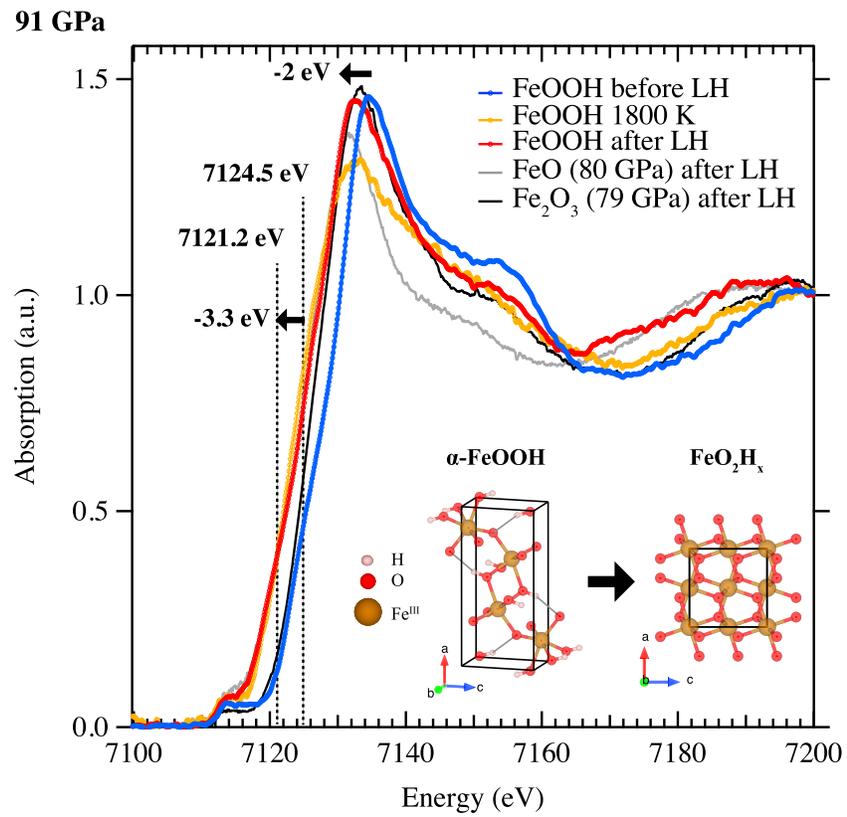
Figure 3. Normalized Fe-K edge XANES spectra collected at ~90 GPa before, during, and after laser heating (LH) of FeOOH loaded into KCl. For comparison, spectra collected in FeO and Fe_2O_3 at similar pressure after laser heating are also represented. A shift of -3.3 eV of the Fe K-edge is observed as α-FeOOH transformed into FeO_2H_x. Hydrogen atoms are not represented in the crystal structure of the FeO_2H_x.

et al., 2017, 2016; Lu & Chen, 2018; Nishi et al., 2017). We thus propose that the present study provides experimental evidence of ferrous iron in pyrite-structured FeO_2H_x.

The possibility of stabilizing ferrous iron in oxygen-rich compositions (as goethite or hematite) had been previously proposed based on structural data obtained by X-ray diffraction (e.g., Hu et al., 2016; Mao et al., 2017). Here we report the first direct spectroscopic evidence of this valence state of iron in such oxygen-rich compositions at P–T conditions achievable both in very cold and hot descending slabs in the lower mantle (Figure 4). This observation will have to be taken into account for modeling the oxygen fugacity, that is, redox state of the Earth's lower mantle which is usually based on the Fe^{3+}/Fe^{2+} ratios. The O_2^{2-}/O^{2-} redox couple which likely interacts with Fe^{3+}/Fe^{2+} will most likely have to be taken into account as well.

Furthermore, according to reaction (1), production of ferrous iron in FeO_2H_x is linked to dehydrogenation of FeOOH when x > 1. In this case, hydrogen atoms will be released as zero-valent (H^0) such as in H_2. For example, at least 60% of the hydrogen atoms initially present in goethite from a subducting banded iron formation (Dobson & Brodholt, 2005) would be released as H^0 (Boulard et al., 2018; Hu et al., 2017; Zhu et al., 2017). This process differs from the release of hydrogen as H^+, often as H_2O, when heating H-bearing mantle minerals. Unlike H_2O, H_2 may be dissolved in lower mantle silicates (Yang et al., 2016). H^0, in whatever form, may also ascend to Earth's surface through the mantle, thus completing a reduced loop of the hydrogen cycle. H^0 may also react with other volatiles, giving rise, for example, to hydrocarbons, thus impacting the carbon oxidation state in the lower mantle and the associated deep carbon cycle. In particular, interaction of these newly discovered iron oxides with CO_2 might change the hydrogen cycle (Boulard et al., 2018); more generally, their evolution in a volatile-bearing silicate lithology should be further studied.

Subduction of FeOOH is geophysically relevant (e.g., Dobson & Brodholt, 2005) but might be limited due to possible dehydration of goethite at shallow depth (e.g., Gleason et al., 2008). However, crystalline-bounded
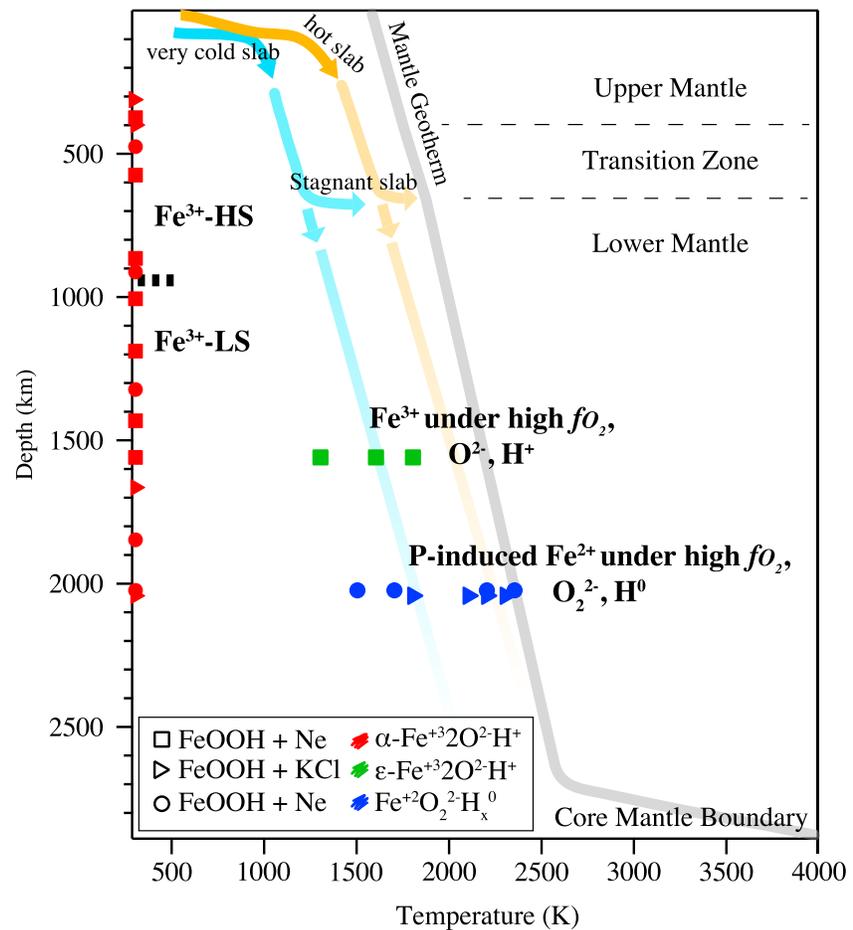
Figure 4. Pressure-induced change of valence state of Fe, O, and H in the lower mantle. FeO_2H_x is likely to be produced in descending slabs that transport hydrated material and where oxidizing conditions exist. Model paths of the hottest (orange) and coldest (blue) slabs from Syracuse et al. (2010) are represented by arrows and their hypothetical extrapolation (orange and blue lines). Mantle geotherm is after Ono (2008).

water almost certainly survive shallow subduction and is recycled to large depth, particularly in cold slabs (Van Keken et al., 2011). Therefore, reactions between iron and water are likely even at lower mantle conditions and the present study on FeOOH transformations is relevant for modeling these interactions at depth. Moreover, other contexts than subduction generate a broad geophysical interest for studying the Fe–O–H system at high pressure. Pyrite-structured FeO_2H_x was indeed reported to result from the reaction of water with metallic iron (Liu et al., 2017; Mao et al., 2017; Yuan et al., 2018), a reaction that may have taken place during core formation resulting in the delivery of hydrogen to the Earth's core (Yuan et al., 2018). Iron hydride FeH_x indeed satisfies density and sound velocities constraints in the Earth's core (e.g., Tagawa et al., 2016). In addition, dehydration melting of transition zone materials swept down to the lower mantle by mantle convection or melting of dense hydrous magnesium phases in subducting slabs that are stagnating near 660-km seismic discontinuity could produce deep hydrous melts at the top of the lower mantle. Reaction of these deep hydrous melt with the metallic iron-rich lower mantle material (Frost et al., 2004) may produce FeO_2H_x in the lower mantle (Yuan et al., 2018). The dense FeO_2H_x peroxide-bearing phase would sink to the core-mantle boundary where it would accumulate. In any case, large amount of FeO_2H_x could be produced at the core-mantle boundary when residual hydrated subducted materials meet metallic iron-rich outer core (Mao et al., 2017). Sound velocity measurement on FeO_2H_x at the core-mantle boundary pressure conditions show that a mixture of FeO_2H_x with the ambient mantle could be a good candidate for the distinct ultralow-velocity zone (Liu et al., 2017). Moreover, a $(Mg,Fe)O_2H_x$ solid solution would reduce the density such that ultralow-velocity

zone might be entirely composed of Mg-bearing pyrite structured FeO_2H_x (Liu et al., 2017). This solid solution has not yet been tested; however Lobanov et al. (2015) have shown that a magnesium peroxide (MgO_2) is stable at the pressure–temperature conditions of the lowermost mantle. Beyond the pure FeOOH stoichiometry the actual valence of iron in realistic lower mantle complex compositions and the resulting physical properties must now be explored.

References

Akahama, Y., & Kawamura, H. (2004). High-pressure Raman spectroscopy of diamond anvils to 250 GPa: Method for pressure determination in the multimegabar pressure range. *Journal of Applied Physics*, *96*(7), 3748–3751. https://doi.org/10.1063/1.1778482

Badro, J., Fiquet, G., Struzhkin, V., Somayazulu, M., Mao, H., Shen, G., & Le Bihan, T. (2002). Nature of the high-pressure transition in Fe_2O_3 hematite. *Physical Review Letters*, *89*(20), 11–14. https://doi.org/10.1103/PhysRevLett.89.205504

Benedetti, L. R., & Loubeyre, P. (2004). Temperature gradients, wavelength-dependent emissivity, and accuracy of high and very-high temperatures measured in the laser-heated diamond cell. *High Pressure Research*, *24*(4), 423–445. https://doi.org/10.1080/08957950412331331718

Boccato, S., Torchio, R., Kantor, I., Morard, G., Anzellini, S., Giampaoli, R., et al. (2017). The melting curve of nickel up to 100 GPa explored by XAS. *Journal of Geophysical Research: Solid Earth*, *122*, 9921–9930. https://doi.org/10.1002/2017JB014807

Boubnov, A., Lichtenberg, H., Mangold, S., & Grunwaldt, J. D. (2015). Identification of the iron oxidation state and coordination geometry in iron oxide- and zeolite-based catalysts using pre-edge XAS analysis. *Journal of Synchrotron Radiation*, *22*, 410–426. https://doi.org/10.1107/S1600577514025880

Boulard, E., Guyot, F., Menguy, N., Corgne, A., Auzende, A., Perrillat, J., & Fiquet, G. (2018). CO_2-induced destabilization of pyrite-structured FeO_2H_x in the lower mantle. *National Science Review*, *5*, 870–877. https://doi.org/10.1093/nsr/nwy032

Bykova, E., Dubrovinsky, L., Dubrovinskaia, N., Bykov, M., McCammon, C., Ovsyannikov, S. V., et al. (2016). Structural complexity of simple Fe_2O_3 oxide at high pressures and temperatures. *Nature Communications*, *7*, 10661. https://doi.org/10.1038/ncomms10661

Dewaele, A., Datchi, F., Loubeyre, P., & Mezouar, M. (2008). High pressure–high temperature equations of state of neon and diamond. *Physical Review B*, *77*, 1–9. https://doi.org/10.1103/PhysRevB.77.094106

Dobson, D. P., & Brodholt, J. P. (2005). Subducted banded iron formations as a source of ultra-low velocity zones at the core-mantle boundary. *Nature*, *434*(7031), 371–374. https://doi.org/10.1038/nature03430

Dräger, G., Frahm, R., Materlik, G., & Brümmer, O. (1988). On the multipole character of the X-ray transitions in the pre-edge structure of Fe K absorption spectra. An experimental study. *Physica Status Solidi B*, *146*(1), 287–294. https://doi.org/10.1002/pssb.2221460130

England, J., Bigelow, J. O., Van Heuvelen, K. M., Farquhar, E. R., Martinho, M., Meier, K. K., et al. (2014). An ultra-stable oxoiron (iv) complex and its blue conjugate base. *Chemical Science*, *5*, 1204–1215. https://doi.org/10.1039/c3sc52755g

Fischer, R. A., Campbell, A. J., Lord, O. T., Shofner, G. A., Dera, P., & Prakapenka, V. B. (2011). Phase transition and metallization of FeO at high pressures and temperatures. *Geophysical Research Letters*, *38*, L24301. https://doi.org/10.1029/2011GL049800

Frost, D. J., Liebske, C., Langenhorst, F., McCammon, C. a., Trønnes, R. G., & Rubie, D. C. (2004). Experimental evidence for the existence of iron-rich metal in the Earth's lower mantle. *Nature*, *428*(6981), 409–412. https://doi.org/10.1038/nature02413

Galoisy, L., Calas, G., & Arrio, M. A. (2001). High-resolution XANES spectra of iron in minerals and glasses: Structural information from the pre-edge region. *Chemical Geology*, *174*(1–3), 307–319. https://doi.org/10.1016/S0009-2541(00)00322-3

Giampaoli, R., Kantor, I., Mezouar, M., Boccato, S., Rosa, A. D., Torchio, R., et al. (2018). Measurement of temperature in the laser heated diamond anvil cell: Comparison between reflective and refractive optics. *High Pressure Research*, *38*, 250–269. https://doi.org/10.1080/08957959.2018.1480017

Gleason, A. E., Jeanloz, R., & Kunz, M. (2008). Pressure-temperature stability studies of FeOOH using X-ray diffraction. *American Mineralogist*, *93*(11–12), 1882–1885. https://doi.org/10.2138/am.2008.2942

Gleason, A. E., Quiroga, C. E., Suzuki, A., Pentcheva, R., & Mao, W. L. (2013). Symmetrization driven spin transition in ε-FeOOH at high pressure. *Earth and Planetary Science Letters*, *379*, 49–55. https://doi.org/10.1016/j.epsl.2013.08.012

Hu, Q., Kim, D. Y., Liu, J., Meng, Y., Yang, L., Zhang, D., et al. (2017). Dehydrogenation of goethite in Earth's deep lower mantle. *Proceedings of the National Academy of Sciences of the United States of America*, *114*, 1498–1501. https://doi.org/10.1073/pnas.1620644114

Hu, Q., Kim, D. Y., Yang, W., Yang, L., Meng, Y., Zhang, L., & Mao, H. K. (2016). FeO_2 and FeOOH under deep lower-mantle conditions and Earth's oxygen-hydrogen cycles. *Nature*, *534*, 241–244. https://doi.org/10.1038/nature18018

Jang, B. G., Kim, D. Y., & Shim, J. H. (2017). Metal-insulator transition and the role of electron correlation in FeO_2. *Physical Review B*, *95*(7), 075144. https://doi.org/10.1103/PhysRevB.95.075144

Kantor, I., Labiche, J. C., Collet, E., Siron, L., Thevenin, J. J., Ponchut, C., et al. (2014). A new detector for sub-millisecond EXAFS spectroscopy at the European Synchrotron Radiation Facility. *Journal of Synchrotron Radiation*, *21*, 1240–1246. https://doi.org/10.1107/S1600577514014805

Kantor, I., Marini, C., Mathon, O., & Pascarelli, S. (2018). A laser heating facility for energy-dispersive X-ray absorption spectroscopy a laser heating facility for energy-dispersive X-ray absorption spectroscopy. *Review of Scientific Instruments*, *89*(1), 013111. https://doi.org/10.1063/1.5010345

Koigstein, M., Richard, C., & Catlow, A. (1998). Ab initio quantum mechanical study of the structure and stability of the alkaline earth metal oxides and peroxides. *Journal of Solid State Chemistry*, *140*(1), 103–115. https://doi.org/10.1006/jssc.1998.7871

Lavina, B., Dera, P., Kim, E., Meng, Y., Downs, R. T., Weck, P. F., et al. (2011). Discovery of the recoverable high-pressure iron oxide Fe_4O_5. *Proceedings of the National Academy of Sciences of the United States of America*, *108*(42), 17281–17285. https://doi.org/10.1073/pnas.1107573108

Lavina, B., & Meng, Y. (2015). Unraveling the complexity of iron oxides at high pressure and temperature: Synthesis of Fe_5O_6. *Science Advances*, *1*(5), e1400260. https://doi.org/10.1126/sciadv.1400260

Liu, J., Hu, Q., Young Kim, D., Wu, Z., Wang, W., Xiao, Y., et al. (2017). Hydrogen-bearing iron peroxide and the origin of ultralow-velocity zones. *Nature*, *551*(7681), 494–497. https://doi.org/10.1038/nature24461

Lobanov, S. S., Zhu, Q., Holtgrewe, N., Prescher, C., Prakapenka, V. B., Oganov, A. R., & Goncharov, A. F. (2015). Stable magnesium peroxide at high pressure. *Scientific Reports*, *5*(1). https://doi.org/10.1038/srep13582

Lu, C., & Chen, C. (2018). Theory high-pressure evolution of crystal bonding structures and properties of FeOOH. *The Journal of Physcial Chemistry.*, *9*, 2181–2185. https://doi.org/10.1021/acs.jpclett.8b00947

Mao, H., Hu, Q., Yang, L., Liu, J., Kim, D. Y., Meng, Y., et al. (2017). When water meets iron at Earth's core-mantle boundary. *National Science Review*, *4*, 870–878. https://doi.org/10.1093/nsr/nwx109

Mao, H., Shu, J., Fei, Y., Hu, J., & Hemley, R. J. (1996). The wustite enigma. *Physics of the Earth and Planetary Interiors*, *96*(2-3), 135–145. https://doi.org/10.1016/0031-9201(96)03146-9

Narygina, O., Mattesini, M., Kantor, I., Pascarelli, S., Wu, X., Aquilanti, G., et al. (2009). High-pressure experimental and computational XANES studies of (Mg,Fe)(Si,Al)O₃ perovskite and (Mg,Fe)O ferropericlase as in the Earth's lower mantle. *Physical Review B*, *79*, 174115. https://doi.org/10.1103/PhysRevB.79.174115

Nishi, M., Kuwayama, Y., Tsuchiya, J., & Tsuchiya, T. (2017). The pyrite-type high-pressure form of FeOOH. *Nature*, *547*(7662), 205–208. https://doi.org/10.1038/nature22823

Ono, S. (2008). Experimental constraints on the temperature profile in the lower mantle. *Physics of the Earth and Planetary Interiors*, *170*(3–4), 267–273. https://doi.org/10.1016/j.pepi.2008.06.033

Ozawa, H., Hirose, K., Tateno, S., Sata, N., & Ohishi, Y. (2010). Phase transition boundary between B1 and B8 structures of FeO up to 210 GPa. *Physics of the Earth and Planetary Interiors*, *179*(3–4), 157–163. https://doi.org/10.1016/j.pepi.2009.11.005

Pascarelli, S., Mathon, O., Mairs, T., Kantor, I., Agostini, G., Strohm, C., et al. (2016). The time-resolved and extreme-conditions XAS (Texas) facility at the European Synchrotron Radiation Facility: The energy-dispersive X-ray absorption spectroscopy beamline ID24. *Journal of Synchrotron Radiation*, *23*(1), 353–368. https://doi.org/10.1107/S160057751501783X

Pernet, M., Joubert, J. C., & Berthet-Colominas, C. (1975). Etude par diffraction neutronique de la forme haute pression de FeOOH. *Solid State Communications*, *17*(12), 1505–1510. https://doi.org/10.1016/0038-1098(75)90983-7

Piquer, C., Laguna-Marco, M. A., Roca, A. G., Boada, R., Guglieri, C., & Chaboy, J. (2014). Fe K-edge X-ray absorption spectroscopy study of nanosized nominal magnetite. *Journal of Physical Chemistry C*, *118*, 1332–1346. https://doi.org/10.1021/jp4104992

Reagan, M. M., Gleason, A. E., Daemen, L., Xiao, Y., & Mao, W. L. (2016). High-pressure behavior of the polymorphs of FeOOH. *American Mineralogist*, *101*, 1483–1488. https://doi.org/10.2138/am-2016-5449

Rohde, J. U., Torelli, S., Shan, X., Mi, H. L., Klinker, E. J., Kaizer, J., et al. (2004). Structural insights into nonheme alkylperoxoiron (III) and oxoiron (IV) intermediates by X-ray absorption spectroscopy. *Journal of the American Chemical Society*, *126*(51), 16750–16761. https://doi.org/10.1021/ja047667w

Sanson, A., Kantor, I., Cerantola, V., Irifune, T., Carnera, A., & Pascarelli, S. (2016). Local structure and spin transition in Fe₂O₃ hematite at high pressure. *Physical Review B*, *94*, 014112. https://doi.org/10.1103/PhysRevB.94.014112

Sinmyo, R., Bykova, E., Ovsyannikov, S. V., McCammon, C., Kupenko, I., Ismailova, L., & Dubrovinsky, L. (2016). Discovery of Fe₇O₉: A new iron oxide with a complex monoclinic structure. *Scientific Reports*, *6*. https://doi.org/10.1038/srep32852

Streltsov, S. S., Shorikov, A. O., Skornyakov, S. L., Poteryaev, A. I., & Khomskii, D. I. (2017). Unexpected 3+ valence of iron in FeO₂, a geologically important material lying "in between" oxides and peroxides. *Scientific Reports*, *7*(1, 13005. https://doi.org/10.1038/s41598-017-13312-4)

Suzuki, A. (2010). High-pressure X-ray diffraction study of ε-FeOOH. *Physics and Chemistry of Minerals*, *37*(3), 153–157. https://doi.org/10.1007/s00269-009-0319-x

Syracuse, E. M., van Keken, P. E., Abers, G. A., Suetsugu, D., Editor, G., Bina, C., et al. (2010). The global range of subduction zone thermal models. *Physics of the Earth and Planetary Interiors* https://doi.org/10.1016/j.pepi.2010.02.004, *183*, 73–90.

Tagawa, S., Ohta, K., Hirose, K., Kato, C., & Ohishi, Y. (2016). Compression of Fe-Si-H alloys to core pressures. *Geophysical Research Letters*, *43*, 3686–3692. https://doi.org/10.1002/2016GL068848

Van Keken, P. E., Hacker, B. R., Syracuse, E. M., & Abers, G. A. (2011). Subduction factory: 4. Depth-dependent flux of H₂O from subducting slabs worldwide. *Journal of Geophysical Research*, *116*, B01401. https://doi.org/10.1029/2010JB007922

Wang, S., Mao, W. L., Sorini, A. P., Chen, C., Devereaux, T. P., Ding, Y., et al. (2010). High-pressure evolution of Fe₂O₃ electronic structure revealed by X-ray absorption. *Physical Review B*, *82*, 144428. https://doi.org/10.1103/PhysRevB.82.144428

Waychunas, G. A., Apted, M. J., & Brown, G. E. (1983). X-ray K-edge absorption spectra of Fe minerals and model compounds: Near-edge structure. *Physics and Chemistry of Minerals*, *10*(1), 1–9. https://doi.org/10.1007/BF01204319

Wilke, M., Farges, F., Petit, P. E., Brown, G. E., & Martin, F. (2001). Oxidation state and coordination of Fe in minerals: An FeK-XANES spectroscopic study. *American Mineralogist*, *86*(5–6), 714–730. https://doi.org/10.2138/am-2001-5-612

Wilke, M., Partzsch, G. M., Bernhardt, R., & Lattard, D. (2005). Determination of the iron oxidation state in basaltic glasses using XANES at the K-edge. *Chemical Geology*, *220*(1-2), 143–161. https://doi.org/10.1016/j.chemgeo.2005.03.004

Xu, W., Greenberg, E., Rozenberg, G. K., Pasternak, M. P., Bykova, E., Boffa-Ballaran, T., et al. (2013). Pressure-induced hydrogen bond symmetrization in iron oxyhydroxide. *Physical Review Letters*, *111*(17). https://doi.org/10.1103/PhysRevLett.111.175501

Yang, X., Keppler, H., & Li, Y. (2016). Molecular hydrogen in mantle minerals. *Geochemical Perspectives Letters*, *2*, 160–168. https://doi.org/10.7185/160geochemlet.1616

Yuan, L., Ohtani, E., Ikuta, D., Kamada, S., Tsuchiya, J., Naohisa, H., et al. (2018). Chemical reactions between Fe and H₂O up to megabar pressures and implications for water storage in the Earth's mantle and core. *Geophysical Research Letters*, *45*, 1330–1338. https://doi.org/10.1002/2017GL075720

Zhu, S. C., Hu, Q., Mao, W. L., Mao, H. K., & Sheng, H. (2017). Hydrogen-bond symmetrization breakdown and dehydrogenation mechanism of FeO₂H at high pressure. *Journal of the American Chemical Society*, *139*, 12,129–12,132. https://doi.org/10.1021/jacs.7b06528